Received: 22 June 2022 | Revised: 10 October 2022 | Accepted: 7 November 2022

DOI: 10.1002/jor.25481

RESEARCH ARTICLE

Journal of Orthopaedic Research®

Influence of bone morphology and femur preparation method on the primary stability of hip revision stems

Tobias Konow[1] | Peter J. Schlieker[1] | Frank Lampe[2] | Benjamin Ondruschka[3] | Michael M. Morlock[1] | Gerd Huber[1]

[1]Institute of Biomechanics, TUHH Hamburg University of Technology, Hamburg, Germany

[2]Schön Klinik Hamburg Eilbek, Hamburg, Germany

[3]Institute of Legal Medicine, University Medical Center Hamburg-Eppendorf, Hamburg, Germany

Correspondence

Tobias Konow, Institute of Biomechanics, TUHH Hamburg University of Technology, Denickestraße 15, 21073 Hamburg, Germany.
Email: tobias.konow@tuhh.de

Abstract

Aseptic loosening is one of the major reasons for re-revisions of cementless revision stems. Insufficient primary stability is associated with bone characteristics and the surgical process. This study aimed to investigate how femur morphology and preparation methods influence the primary stability of revision stems. The Femur morphology was described by the upper femoral curvature (UFC) and an individualized Dorr type classification based on the ratio between the canal-to-calcar ratio (CCR*) and the cortical index (CI*) introduced as the cortical-canal shape (CCS). Manual and powered reaming in combination with helical and straight reamers were used to prepare the bone cavity of 10 cadaveric human femur pairs. Forces during stem impaction were recorded (Reclaim, Depuy Synthes). Micromotion at the bone–implant interface during cyclic axial loading and torsional load to failure was determined. The CCS and impaction forces ($R^2 = 0.817$, $p < 0.001$) or torsional strength ($R^2 = 0.577$, $p < 0.001$) are inversely related. CCS did not correlate with micromotion during axial loading ($R^2 = 0.001$, $p > 0.999$), but proximal femoral curvature did ($R^2 = 0.462$, $p = 0.015$). Powered reaming and straight reamers led to an improved torsional strength (both: $p = 0.043$). The Individualized Dorr classification CCS and UFC allows a good estimation of the primary stability of revision stems. For severely curved Dorr type-C femurs, an alternative anchorage method should be considered clinically.

KEYWORDS

bone morphology, canal reaming, Dorr type, femur curvature, primary stability, revision THA

1 | INTRODUCTION

Primary total hip arthroplasty (THA) exhibits success rates above 96% within the first 5 years.[1–3] Changing demographics come along with increasing physical activities among older patients and increased expectations for life quality. Hence, the worldwide number of primary THA and revision procedures is also increasing,[4] especially in the elderly.[2] With aging and consecutive interventions, the bone quality and the remaining bone stock decline,[5–9] and surgeons can not rely on the proximal trabecular bone structure.[10] Tapered revision stems, anchoring distally in the diaphysis, become the preferred choice of the surgeon.[11–13] The majority of re-revisions are caused by aseptic loosening—potentially introduced by excessive micromotion between stem and bone.[14–17] In particular, stem subsidence occurs frequently

with cementless revision stems.[18,19] Postoperative stem subsidence less than 2 mm[20] and micromotions of less than 30 µm are considered harmless,[21,22] while micromotions >150 µm are considered an unfavorable condition for osseointegration.[23]

Patient-related factors such as femur shape or bone quality but also upper femoral curvature (UFC) may have an impact on the primary stability of cementless revision stems. Bone quality and decreased femoral strength are often age-related[24] and associated with comorbidities.[25] Macroscopically, the femoral morphology is usually described by the Dorr type.[26] Femurs of young, active patients often have a funnel-shaped medullary cavity with a thick cortex categorized as Dorr type A. Femurs with a stove-piped shaped canal and a thin cortex—common in the elderly[27]—are assigned to Dorr type C. Since revision stems are anchored in the diaphysis, the cortical morphology of the femur influences the stability. Dorr type C bones with reduced bone strength often require stems with larger diameters.[27] Preoperative determining of the bone morphology according to the Dorr type is important for planning but usually is only performed qualitatively. Dorr's classification either refers to the canal-to-calcar ratio (CCR) or the cortical index (CI), determined at fixed positions without considering body-specific factors such as patient height,[26,28] and an ideal AP or ML view orientation cannot be guaranteed. Furthermore, using the CCR or the CI does not necessarily yield the same Dorr type for a specific femur, which makes a unique classification impossible in some cases. Combined, this can lead to ambiguous results even for the most experienced surgeons.[29,30] A unique classification to evaluate the morphology of the proximal femur based on the original work of Dorr is desirable to support surgeons' implant choices and to elucidate differences in clinical outcomes.

In addition to proximal femur morphology, especially important for elderly,[2] the cavity preparation method bears the potential to influence the outcome of the procedure. Likewise, in primary THA, where preparation affects stem seating for low bone mineral density (BMD),[31] broach design influenced the shape of the cavity,[31] this could also apply to the reamer design in revision THA. Furthermore, manual reaming could cause more variable cavities compared to powered reaming. However, the effect of these factors on the primary stability of revision stems has not been fully investigated.

This study aimed to investigate how femur morphology and preparation methods influence the primary stability of revision stems.

2 | METHODS

Ten femur pairs from human donors (7 female, 3 male, 74.8 ± 6.1 years, range 65–84 years) were excised post-mortem and stored below −20°C.[32] The Ethics Commission of the Medical Association Hamburg (WF-067/18) approved this study.

2.1 | Femur analysis

CT scans (Brilliance 16, Philips) with a calibration phantom (QSA, QRM) were taken (voxel size: 0.5 × 0.5 × 0.5 mm^3) and Hounsfield units were converted to BMD in terms of Calcium-Hydroxyapatite per milliliter (Structural Insight 3, University Medical Center Schleswig-Holstein[33]). The BMD of the cortical bone was determined at a 10 mm wide ring of the femur shaft, 100 mm below the trochanter minor (threshold: [500, 1500 mgHA/cm^3]; AVIZOLite 9.7.0, Thermo Fisher Scientific). The cortical bone and medullary canals were segmented based on thresholds (cortical bone: 500–1500 mgHA/cm^3; medullary canal: −250 to 500 mgHA/cm^3).[31] CT data were pre-aligned based on the homogeneously distributed point cloud of the cortical shell using its three main principal components (Matlab 2020b, The MathWorks).

Percentages of donors' body height (BH) were used as body-specific measures for femur classification. The anatomical femur axis was defined by a best-fit line through the diaphysis between 2% BH ($z_{2\%}$) and 8% BH ($z_{8\%}$) distally to the trochanter minor (TM). This femur section was further divided into two equal sub-sections ($z_{2\%}$ to $z_{5\%}$ and $z_{5\%}$ to $z_{8\%}$) and used to determine the UFC (β) as the angle between the respective canal axes of the sub-sections (Figure 1A).

Individual body-height-specific femur types CCR* and CI* (* stands for the individualized adapted method) on the bases of Dorr et al.[26] were determined, by replacing the fixed positions of 30 mm (z_{30mm}) and 100 mm (z_{100mm}) below the TM with body-specific measures of 1.7% BH ($z_{1.7\%}$) and 5.8% BH ($z_{5.8\%}$). Positions are the same for an average German body height of 172 cm[34] (Figure 1B, Equation 1).

$$CI = \frac{D_{cort,100mm} - D_{im,100mm}}{D_{cort,100mm}} = 1 - \frac{D_{im,100mm}}{D_{cort,100mm}} \overset{BH}{\Rightarrow} 1 - \frac{D_{im,5.8\%}}{D_{cort,5.8\%}} \quad (1)$$

AP and ML (Lauenstein) radiographs were replaced by cross-sectional areas of the cortical shell (A_{cort}) and the intramedullary canal (A_{im}) determined from CT data. Equation (1) refers to the diameter that is available in the x-ray projection. In CT images, however, the cross-sectional area is available, which is roughly proportional to the square of the diameter. Hence, the individualized CI* was determined from the medullary cross-sectional area $A_{im,5.8\%}$ and the cortical cross-sectional area $A_{cort,5.8\%}$ (Figure 1B; Equation 2).

$$CI^* = 1 - \sqrt{\frac{A_{im,5.8\%}}{A_{cort,5.8\%}}} \quad (2)$$

To describe the conical shape of the intramedullary canal, the originally fixed positions to determine the canal diameters at 30 mm ($D_{im,30mm}$) and 100 mm below the TM ($D_{im,100mm}$) were expressed as a percentage of the body height (Equation 3).

$$CCR = \frac{D_{im,100mm}}{D_{im,TM}} = \frac{7}{10 \cdot \frac{D_{im,30mm}}{D_{im,100mm}} - 3} \overset{BH}{\Rightarrow} \frac{7}{10 \cdot \frac{D_{im,1,7\%}}{D_{im,5.8\%}} - 3} \quad (3)$$

Inline with the former, the individual CCR* was determined with cross-sectional areas instead of diameters (Figure 1B, Equation 4).

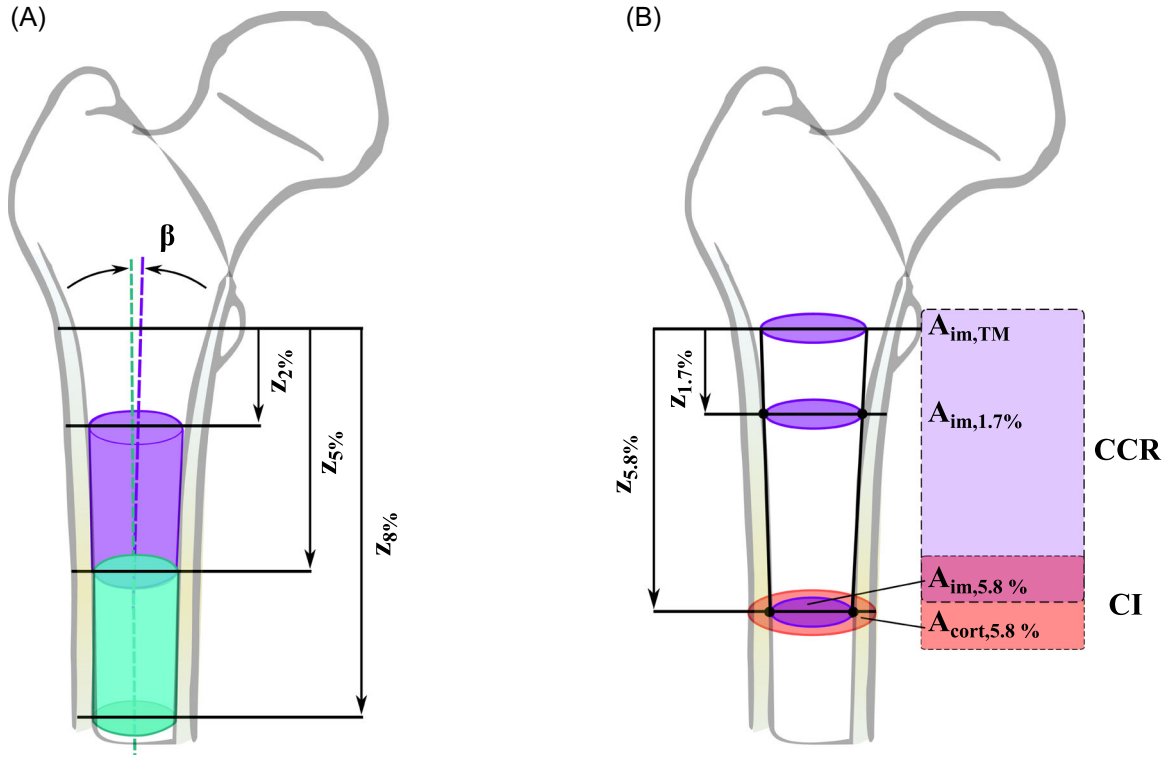

FIGURE 1 (A) Parameters used to determine the upper femur curvature (UFC). The respective curvature was derived as the angel (β) between the canal axes of a proximal (2%–5% of body height below the trochanter minor) and a further distal section (5%–8% of body height below the trochanter minor) of the femural canal. (B) Body-height-specific parameters used to compute the individual cortical index (CI*) and the canal-to-calcar ratio (CCR*). The intramedullary areas (A_{im}) are indicated by purple circles at the respective positions (z). The area of the cortical shell (A_{cort}) is indicated by an orange circle. [Color figure can be viewed at wileyonlinelibrary.com]

FIGURE 2 Representative illustration of the Reclaim stem. In the sectional view, the profile with eight vertical fins is visible.

$$CCR^* = \frac{7}{10 \cdot \sqrt{\frac{A_{im,1.7\%}}{A_{im,5.8\%}}} - 3} \quad (4)$$

The ratio between CCR* and CI* (CCR*/CI*) is further referred to as the cortical-canal shape (CCS) and is used to evaluate the in-vitro experiments.

2.2 | In-vitro experiment

Revision stems (Reclaim Revision Hip System, stem-length: 140 mm; Depuy Synthes; Figure 2) were implanted by one experienced surgeon using different cavity preparation methods. First, the drive method for reaming was varied, with manual reaming on one femur (n = 5) and powered reaming on the contralateral femur (n = 5) using helical reamers. Second, standard helical reamers (n = 5) were used on one and straight reamers (n = 5) on the contralateral femur both with powered mode. During cavity preparation, reamer diameters were stepwise increased (1 mm) until the surgeon perceived sufficient stability. The final depth and position of the reamer were measured with respect to the greater trochanter by a digitalized caliper.

Afterward, specimens were embedded (Technovit 4004, Kulzer GmbH) aligned with the reamer axis. Stems were implanted using a drop tower with subsequently stepwise increasing energy (10 impactions at 3 J and 5 impactions at 4, 5, 6, and 7 J each) until the desired stem position (as reamed) was reached (Figure 3A). In case the intended stem position could not be achieved after this protocol, implantation was discontinued. Impaction forces (Kistler 9333A) and the implantation depth per impact were recorded.

Specimens were mounted with the implant axis aligned from joint center to joint center of two Cardan joints (Figure 3B). Primary

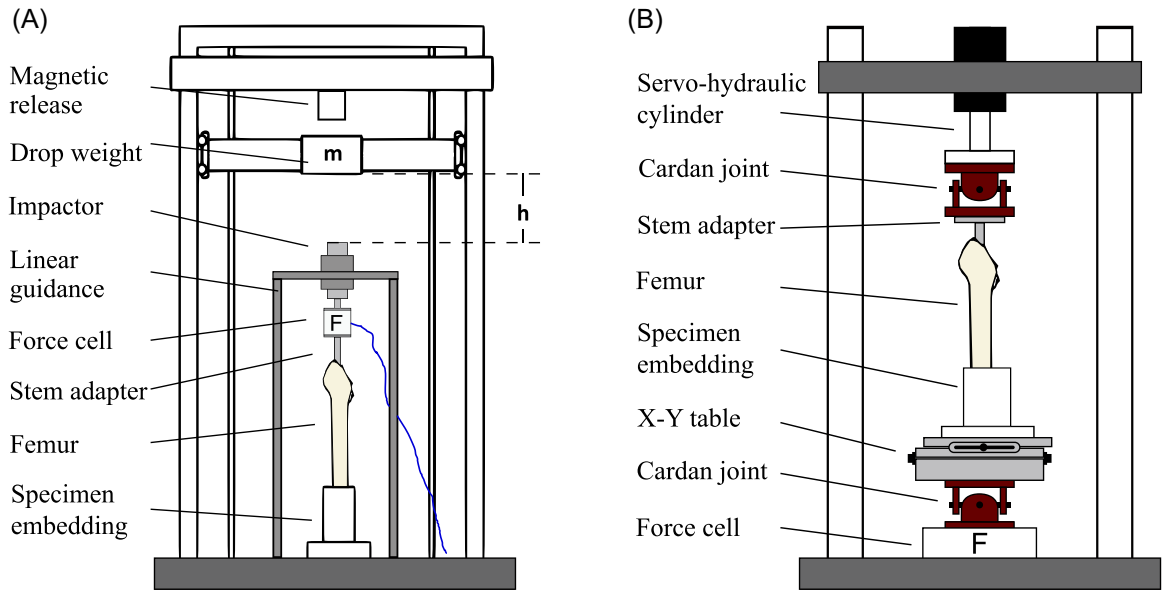

FIGURE 3 (A) Schematic display of the drop tower used for stem impaction. Dynamic impaction forces were recorded with a dynamic load cell. (B) Schematic display of the experimental setup in the servo-hydraulic testing device. A torque-free load transmission was possible through the use of two Cardan joints. [Color figure can be viewed at wileyonlinelibrary.com]

stability was determined during force-controlled cyclic sinusoidal axial compression load (1 Hz, 200–2000 N, 30 min; Bionix II, MTS). Axial point-to-point micromotion between implant and bone is measured at the proximal head resection area using digital image correlation (DIC, ARAMIS 3D Camera, GOM) at seven definite time points (10 cycles at the beginning and 10 cycles every 300 cycles, 25 fps, measuring volume: $100 \times 80 \times 50\,mm^3$, 2752×2200 pixels, marker diameter 0.4 mm, 5 µm measurement noise). The proximal sections of the distal stems were machined to enable the torsional machine-implant load transfer during the torque-to-failure tests. These changes had no effect on the bone–implant interface. Ultimate torque to failure (angular velocity: 0.5°/s) was determined in combination with a static axial preload (500 N).

2.3 | Statistical analysis

Statistics were performed with a type I error level of 0.05 (SPSS 24.0, SPSS Inc.). Multiple Pearson correlations were used to identify relations between the parameters. Wilcoxon sign-rank analysis was performed to determine effects within paired femurs.

3 | RESULTS

The cortical BMD ($1012.4 \pm 67.3\,mgHA/cm^3$) was the same within femur pairs ($p = 0.970$, $1-\beta = 0.011$) and in both study groups ($p = 0.462$, $1-\beta = 0.110$). A high level of symmetry between femur sides was found regarding the UFC ($p = 0.389$, $1-\beta = 0.066$) and the CCS ($p = 0.954$, $1-\beta = 0.022$). UFC and CCS were also similar for specimens of both study groups ($4.2 \pm 1.3°$, $p = 0.526$, $1-\beta = 0.094$; 1.14 ± 0.18, $p = 0.668$, $1-\beta = 0.070$). Femur length increased with increasing body height ($R^2 = 0.83$, $p < 0.001$).

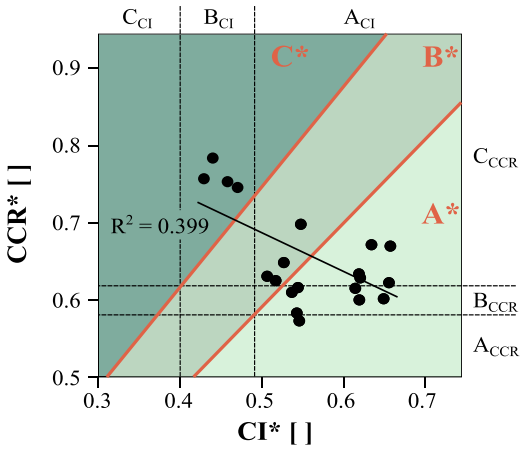

FIGURE 4 The canal-to-calcar ratio (CCR*) as a function of the cortical index (CI*) exhibits a negative correlation ($f(x) = 1-0.5x$; $p = 0.003$). The cutoff limits for the Dorr classification according to the CCR and the CI are indicated in black.[26] The cutoff limits for the modified classification (CCS) are indicated in orange (values are given in Table 1). [Color figure can be viewed at wileyonlinelibrary.com]

Body-specific CCR* yielded results similar to standard Dorr CCR ($p = 0.349$, $1-\beta = 0.148$). Differences were seen with regard to CI* for small patients (<165 cm; $p = 0.043$) and larger patients (>175 cm; $p = 0.028$). In 90% of the observed specimens, the CCR* and the CI* classification led to different Dorr types—alike CCR and CI. A negative correlation between CCR* and CI* ($R^2 = 0.399$, $p = 0.003$; Figure 4) was found. To differentiate between Dorr types A*, B*, and C* Dorr's cutoff limits for the CCR and the CI were applied to the

TABLE 1 Cutoff values for CI, CCR, and CCS to categorize the femurs into Dorr and adjusted Dorr* types[26]

Dorr type[24]	CI	CCR	Dorr type*	CCS
A	>0.49	<0.58	A*	<1.18 (0.58/0.49)
B	[0.40, 0.49]	[0.58, 0.62]	B*	[1.18, 1.54]
C	<0.40	>0.62	C*	>1.54 (0.62/0.40)

Abbreviations: CCR, canal-to-calcar ratio; CI, cortical index; CCS, cortical-canal shape.

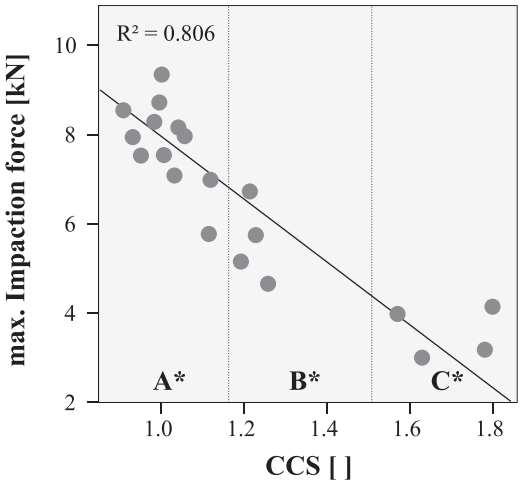

FIGURE 5 Statistically sig. negative correlation between maximum impaction force and the CCS. CCS, cortical-canal shape.

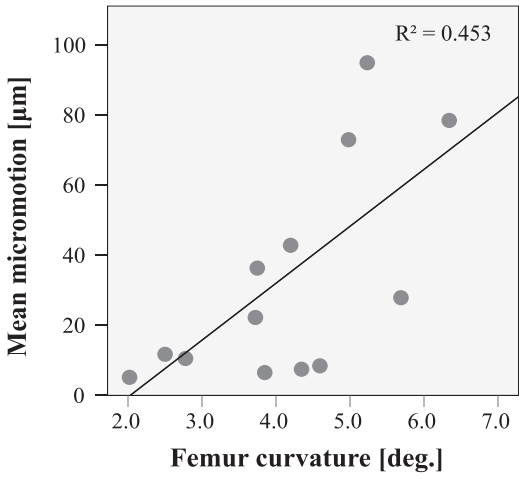

FIGURE 6 Statistically sig. positive correlation between the micromotion and the UFC for specimens exhibiting more than 5 µm of micromotion. UFC, upper femoral curvature.

ratio CCR/CI and CCS, respectively (Table 1[26]). A linear function from the origin through those hereby generated points represents the new cutoff limits (Figure 4). The majority of femurs were assigned to the Dorr type A* (A* = 12, B* = 4, and C* = 4). Patient's height did not correlate with the CCS ($p = 0.588$).

Thirteen implants (65%) were impacted to the desired position while 7 implants (35%) showed an elevated position (Mean elevation: 6.0 ± 3.0 mm). Maximum impaction forces and energies were similar independent of the reaming method (Forces: 6.5 ± 1.9 kN, $p = 0.946$, $1-\beta = 0.068$; Energy: 90.6 ± 50.4 J, $p = 0.830$, $1-\beta = 0.094$). A paired analysis of the isolated subgroups neither revealed differences. UFC neither affected impaction forces ($R^2 = 0.006$, $p = 0.743$, $1-\beta = 0.061$) nor the required impaction energy ($R^2 = 0.003$, $p = 0.805$, $1-\beta = 0.055$). Impaction forces increased with decreasing CCS ($R^2 = 0.806$, $p < 0.001$; Figure 5). Higher demand of impaction energy was associated with decreasing CCS ($R^2 = 0.721$, $p < 0.001$).

Seven specimens (35%) exhibited small cyclic micromotions of less than 5 µm (0.5 ± 2.4 µm; five fully seated, two not fully seated), which is within the noise of the DIC system. Thirteen specimens exhibited reasonable micromotions of 32.7 ± 30.9 µm. Micromotions did neither depend on reaming method ($p = 0.405$, $1-\beta = 0.229$) nor on cortical BMD ($R^2 = 0.096$, $p = 0.183$, $1-\beta = 0.269$) nor on the CCS ($R^2 = 0.019$, $p = 0.552$, $1-\beta = 0.089$). For specimens exhibiting micromotions above 5 µm, a positive correlation was found with increasing UFC ($R^2 = 0.453$, $p = 0.015$; Figure 6). Moreover, micromotions came along with increased stem subsidence ($R^2 = 0.317$, $p = 0.010$), but stem subsidence was found to be small (−10.5 ± 22.7 µm). Bone morphology did not affect stem subsidence (CCS: $R^2 = 0.004$, $p = 0.778$, $1-\beta = 0.057$; UFC: $R^2 = 0.025$, $p = 0.509$, $1-\beta = 0.102$).

Powered reaming resulted in a 21% increased torsional strength compared to manual reaming ($p = 0.043$, $1-\beta = 0.361$, Figure 7B). Straight reamers appeared to be 11% superior compared to helical reamers in terms of torsional strength ($p = 0.043$, $1-\beta = 0.361$; Figure 7B). With a decreasing CCS higher torsional strength was observed ($R^2 = 0.579$, $p < 0.001$; Figure 7A).

4 | DISCUSSION

Specimens of the given cohort have been unaffected by primary implantation and consequently did not have bone defects or losses—unlike those seen in the clinical situation with revision THA. However, proximal bone defects hardly affect the fixation of the stem in the diaphysis and thus the findings are regarded to be transferable. No degenerated bone structures were found with the majority having a CCS below 1.3 (Dorr type A* or B*). Whether the results would be different if more Dorr type C* samples with poor bone quality were included remained unclear. The homogeneity of paired specimens between study groups concerning BMD and CCS indicates that the evaluation of the different preparation methods was not recently influenced by donor-specific anthropometric characteristics. The contact area between bone and implant was found to influence the

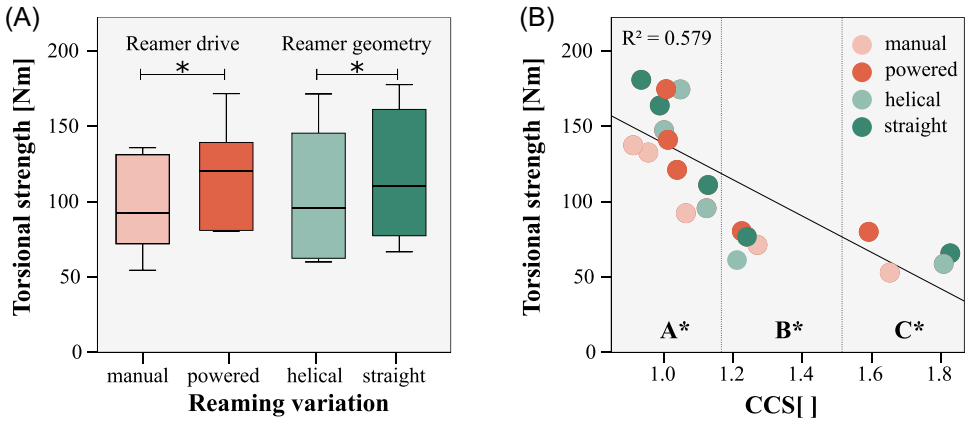

FIGURE 7 (A) Maximum torsional strength regarding the different reaming approaches. Pairwise statistical analysis revealed differences between manual and powered reaming as well as between helical and straight reamers. (B) Decrease in torsional strength with increasing CCS. CCS, cortical-canal shape. [Color figure can be viewed at wileyonlinelibrary.com]

torsional strength.[35] Since the tested stems had only a small difference in stem size (15 ± 1), the contact area was assumed to be similar since the stem-length, the number of vertical fins and their shape was identical. The observed torsional strength within the bone–implant interface was slightly above the loads occurring during high-load activities like jogging.[36]

The use of body-height-specific measures to determine CCR* and CI* is justified by the correlation of BH and femur length found in this study alike to previous ones.[37,38] The body-specific normalization solely results in minor changes for most femurs, but larger or small patients might benefit from this approach. Percentages of donors' body heights with decimal places were used to reflect the constant positions suggested by Dorr and the average BH of the donors' population. However, simplified percentages, for example, 2% and 6% should work similarly. Threshold-based CT detection of cortical and trabecular bone is advantageous compared to 2D projections due to its reproducible results without positioning errors during image acquisitions but requires quantitative CT scans. Since CT scans are recommended before revisions, the patient would not be exposed to additional radiation.[39] The semi-automatic, numerical determination of femoral morphology, additionally improves the inter- and intraobserver reliability deplored in literature[29,30] and could be implemented fully automatically in modern preoperative planning software. The negative correlation between CCR and CI was already mentioned by Dorr et al. but not pursued further.[26] Thus, the Dorr type is often determined by just one parameter, either by CCR or CI with potentially contradictory results, limiting the comparability of different studies. The newly introduced CCS not only describes the correlation between CCR* and CI*, but also serves as a unique measure to quantify femoral morphology, which may positively influence preoperative planning through correct implant selection and might prevent complications during or after revision surgery.

Standard powered reaming appears to be superior compared to the manual approach since it is time-efficient, involves less physical work and yields to higher torsional strength, presumably due to a more uniform cavity. It is uncertain whether straight reamers further improve the junction due to their changed geometry or merely due to the sharper cutting edges caused by the less previous operating time of the reamer.

One-third (35%) of stems exhibited micromotions of less than 5 µm, in the range of the signal noise, and therefore, no correlations between micromotion and CCS or BMD were observed. The lower performance observed in curved femurs in terms of increase in micromotion may be related to a smaller contact area within the less congruent interface, which is known to reduce primary stability.[35] Mechanically, a low CCS with a high BMD ($R^2 = 0.47$, $p = 0.002$), as found in Dorr type A bones, increases system stiffness leading to higher impaction forces and energies which improves primary stability. In contrast, the thin cortex of Dorr type C bones with low BMD, often found in elderly patients most commonly affected by revision THA,[2,27] does not provide comparable radial pressures at the implant–bone interface to achieve similar torsional strength. For these specimens, in particular, the maximum torsional moments are close to loads projected for activities like jogging.[36]

Overall, femur morphology appears worthwhile to be considered during cementless revision THA, because of the exhibited correlation between impaction force, impaction energy, and bone-related parameters (BMD, CCS, and UFC) with primary stability.

5 | CONCLUSION

With the CCS a unique Dorr type* can be determined for any femur. Including body-height-specific measures and a semi-automatic computation of the CCR* and the CI* from three-dimensional CT data improves the reproducibility and reduces inter-/intraobserver variations. The CCS appears to be able to predict the mechanical relationships between bone and implant, and such may support adequate prosthesis selection. Apart from the clinical situation, this

allows objective body-specific femoral morphological parameters to be used for in-vitro analysis. Since micromotion is affected by UFC and torsional stability by CCS, it may be worthwhile to consider both parameters in combination. In contrast to bone morphology, the preparation method plays a minor role for primary stability. Slight advantages of powered compared to manual reaming and the reamer geometry will most likely not decide the revision's success. A combination of several adverse factors may lead to early implant failure and re-revision. In severely curved type C* femurs that have been manually prepared, primary stability could be critically compromised, so an alternative anchorage method may be beneficial for these patients.

AUTHOR CONTRIBUTIONS

Tobias Konow: Study design; methodology; testing; investigation; formal analysis; writing – original draft. **Peter J. Schlieker**: Methodology; writing – original draft. **Frank Lampe**: Implantations. **Benjamin Ondruschka**: Specimen selection; harvesting & imaging. **Michael M. Morlock**: Statistical analysis; writing – review and editing. Gerd Huber: Study design; project coordination; writing – review and editing. All authors have read and approved the submitted manuscript.

ACKNOWLEDGMENTS

The authors would like to thank Depuy Synthes for providing the prosthesis components, surgical tools, and financial support. All experimental studies were performed at the University Medical Center Hamburg-Eppendorf (UKE) and the TUHH Hamburg University of Technology. Open Access funding enabled and organized by Projekt DEAL.

CONFLICTS OF INTEREST

The authors have the following conflicts of interest: FL is a paid consultant of Depuy Synthes and Aesculap. BO is a board member of the German Society of Legal Medicine. MMM is a paid consultant of DePuy Synthes and obtains research support as a Principal Investigator from Ceramtec, DePuy, and Beiersdorf. He obtains speaker's fees from Aesculap, Ceramtec, DePuy, Zimmer, Peter Brehm, Corin, and Mathys and is in the editorial board "Trauma und Berufskrankheit." GH is an associated member of the board of the German Society of Biomechanics.

ORCID

Tobias Konow http://orcid.org/0000-0002-5265-997X

REFERENCES

1. No Authors Listed. Hip, Knee & Shoulder Arthroplasty: Annual Report 2019. AOANJRR. 2019.
2. Grimberg A, Jansson V, Lützner J, et al. Jahresbericht 2021. EPRD Deutsche Endoprothesenregister. 2021.
3. No Authors Listed. Hip, Knee & Shoulder Arthroplasty: Annual Report 2020. AOANJRR. 2020.
4. Kurtz SM, Mowat F, Ong K, et al. Prevalence of primary and revision total hip and knee arthroplasty in the United States from 1990 through 2002. *J Bone Jt Surg Am*. 2005;87(7):1487-1497.
5. Venesmaa PK, Kröger HKJ, Jurvelin JS, Miettinen HJA, Suomalainen OT, Alhava EM. Periprosthetic bone loss after cemented total hip arthroplasty. *Acta Orthop Scand*. 2003;74(1):31-36.
6. Harris W, Schiller A, Scholler J, Freiberg R, Scott R. Extensive localized bone resorption in the femur following total hip replacement. *J Bone Jt Surg*. 1976;58(5):612-618.
7. Dan D, Germann D, Burki H, et al. Bone loss after total hip arthroplasty. *Rheumatol Int*. 2006;26(9):792-798.
8. Harris WH. Wear and periprosthetic osteolysis the problem. *Clin Orthop Relat Res*. 2001;393:66-70.
9. Kang MN, Huddleston JI, Hwang K, Imrie S, Goodman SB. Early outcome of a modular femoral component in revision total hip arthroplasty. *J Arthroplasty*. 2008;23(2):220-225.
10. Amanatullah DF, Howard JL, Siman H, Trousdale RT, Mabry TM, Berry DJ. Revision total hip arthroplasty in patients with extensive proximal femoral bone loss using a fluted tapered modular femoral component. *Bone Jt J*. 2015;97-B:312-317.
11. Böhm P, Bischel O. The use of tapered stems for femoral revision surgery. *Clin Orthop Relat Res*. 2004;420:148-159.
12. Skyttä ET, Eskelinen A, Remes V. Successful femoral reconstruction with a fluted and tapered modular distal fixation stem in revision total hip arthroplasty. *Scand J Surg*. 2012;101(3):222-226.
13. Nadaud MC, Griffin WL, Fehring TK, et al. Cementless revision total hip arthroplasty without allograft in severe proximal femoral defects. *J Arthroplasty*. 2005;20(6):738-744.
14. No Authors Listed. National Joint Registry–17th Annual Report 2020. Natl. Jt. Regist. (December 2019). 2020.
15. Streit MR, Haeussler D, Bruckner T, et al. Early migration predicts aseptic loosening of cementless femoral stems: a long-term study. *Clin Orthop Relat Res*. 2016;474(7):1697-1706.
16. Kassi JP, Heller MO, Stoeckle U, Perka C, Duda GN. Stair climbing is more critical than walking in pre-clinical assessment of primary stability in cementless THA in vitro. *J Biomech*. 2005;38(5):1143-1154.
17. Sundfeldt M, Carlsson LV, Johansson CB, Thomsen P, Gretzer C. Aseptic loosening, not only a question of wear: a review of different theories. *Acta Orthop*. 2006;77(2):177-197.
18. Moreland JR, Bernstein ML. Femoral revision hip arthroplasty with uncemented, porous-coated stems. *Clin Orthop Relat Res*. 1995;319:141-150.
19. Hancock DS, Sharplin PK, Larsen PD, Phillips FT. Early radiological and functional outcomes for a cementless press-fit design modular femoral stem revision system. *HIP Int*. 2019;29(1):35-40.
20. Walker PS, Mai SF, Cobb AG, et al. Prediction of clinical outcome of THR from migration measurements on standard radiographs: a study of cemented Charnley and Stanmorefemoral stems. *J Bone Jt Surg Ser B*. 1995;77(5):705-714.
21. Bragdon CR, Burke D, Lowenstein JD, et al. Differences in stiffness of the interface between a cementless porous implant and cancellous bone in vivo in dogs due to varying amounts of implant motion. *J Arthroplasty*. 1996;11(8):945-951.
22. Kawahara H, Kawahara D, Hayakawa M, Tamai Y, Kuremoto T, Matsuda S. Osseointegration under immediate loading: biomechanical stress-strain and bone formation-resorption. *Implant Dent*. 2003;12(1):61-68.
23. Pilliar RM, Lee JM, Maniatopoulos C. Observations on the effect of movement on bone ingrowth into porous-surfaced implants. *Clin Orthop Relat Res*. 1986;208:108–113.
24. Keaveny TM, Kopperdahl DL, Melton LJ, et al. Age-dependence of femoral strength in white women and men. *J Bone Miner Res Off J Am Soc Bone Miner Res*. 2010;25(5):994-1001.
25. Grynpas M. Age and disease-related changes in the mineral of bone. *Calcif Tissue Int*. 1993;53(Suppl 1):S57-S64.
26. Dorr LD, Faugere M-C, Mackel AM, Gruen TA, Bognar B, Malluche HH. Structural and cellular assessment of bone quality of proximal femur. *Bone*. 1993;14(3):231-242.

27. Toro G, Bothorel H, Saffarini M, Jacquot L, Chouteau J, Rollier JC. Uncemented total hip arthroplasty in octogenarian and nonagenarian patients. *Eur J Orthop Surg Traumatol*. 2019;29(1):103-110.
28. Karayiannis PN, Cassidy RS, Hill JC, Dorr LD, Beverland DE. The relationship between canal diameter and the Dorr classification. *J Arthroplasty*. 2020;35(11):3204-3207.
29. Nakaya R, Takao M, Hamada H, Sakai T, Sugano N. Reproducibility of the Dorr classification and its quantitative indices on plain radiographs. *Orthop Traumatol Surg Res*. 2019;105(1):17-21.
30. Najd Mazhar F, Jafari D, Nojoomi M, Mirzaei A, Tayebi H. Inter and intra-observer reliability of Dorr classification in proximal femur morphology. *Shafa Orthop J*. 2018;5(1): e64801.
31. Bätz J, Messer-Hannemann P, Lampe F, et al. Effect of cavity preparation and bone mineral density on bone-interface densification and bone-implant contact during press-fit implantation of hip stems. *J Orthop Res*. 2019;37(7):1580-1589.
32. Püschel K, Heinemann A, Dietz E, Hellwinkel O, Henners D, Fitzek A. New developments and possibilities in the field of post-mortem medicine mortui vivos docent. *Rechtsmedizin*. 2020;30(6):425-429.
33. Graeff C, Timm W, Nickelsen TN, et al. Monitoring teriparatide-associated changes in vertebral microstructure by high-resolution CT in vivo: results from the EUROFORS study. *J Bone Miner Res*. 2007;22(9):1426-1433.
34. Statistisches Bundesamt. 2018. Mikrozensus–Fragen zur Gesundheit–Körpermaße der Bevölkerung. 2017.49(August):1-17. https://www.destatis.de/DE/Themen/Gesellschaft-Umwelt/Gesundheit/Gesundheitszustand-Relevantes-Verhalten/Publikationen/Downloads-Gesundheitszustand/koerpermasse-5239003179004.html
35. Meneghini RM, Hallab NJ, Berger RA, Jacobs JJ, Paprosky WG, Rosenberg AG. Stem diameter and rotational stability in revision total hip arthroplasty: a biomechanical analysis. *J Orthop Surg*. 2006;1(1):5.
36. Huber G, Morlock MM. Which length should the neck segment of modular revision stems have? *Clin Biomech*. 2022;94:105286.
37. Mahakkanukrauh P, Khanpetch P, Prasitwattanseree S, Vichairat K, Troy Case D. Stature estimation from long bone lengths in a Thai population. *Forensic Sci Int*. 2011;210(1-3):279.e1-279.e7.
38. Baba M, Hyodoh H, Okazaki S, et al. Stature estimation from anatomical landmarks in femur using postmortem CT. *J Forensic Radiol Imaging*. 2016;7:28-32.
39. Kuroda K, Kabata T, Maeda T, et al. The value of computed tomography based navigation in revision total hip arthroplasty. *Int Orthop* 2014;38(4):711-716.

How to cite this article: Konow T, Schlieker PJ, Lampe F, Ondruschka B, Morlock MM, Huber G. Influence of bone morphology and femur preparation method on the primary stability of hip revision stems. *J Orthop Res*. 2022;1-8. doi:10.1002/jor.25481